Affiliation: Independent Researcher *Email:* bierrenbach85@gmail.com

Abstract

This supplement extends the empirical validation of the Regenerative Gravity and Spatial Homeostasis Equation (GRHE), introduced in the main manuscript [1], by testing its redshift predictions across 13 cosmological scenarios, including Type Ia supernovae, baryon acoustic oscillations (BAO), and galaxy clusters. GRHE posits a static universe governed by a scalar field $\Psi(r,t)$ and the golden ratio ($\phi \approx 1.618$). Combined with the seven scenarios in the main manuscript, these 20 tests yield an average error of 1.63%, with 1.11% for cosmological scales, comparable to LambdaCDM's 1–2% error [8]. Results are summarized in Table 1 and visualized in Figures 1 and 2. These findings complement advanced cosmological tests in Supplementary Material V and reinforce GRHE's robustness.

GRHE Supplementary Material I: Empirical Redshift Tests and Cosmological Structures

Jorge Bierrenbach

April 2025

1 Introduction

The Regenerative Gravity and Spatial Homeostasis Equation (GRHE), detailed in the main manuscript [1], reinterprets redshift as a response to a scalar field $\Psi(r,t)$, using the golden ratio ($\phi \approx 1.618$) to unify metrics. Unlike LambdaCDM, which relies on expansion and dark components [8], GRHE posits a static universe in equilibrium. The main manuscript validates GRHE across seven scenarios, achieving a 1.11% error for cosmological scales, extended to 20 scenarios with an overall average error of 1.63% [1]. This supplement tests 13 additional scenarios, from Type Ia supernovae to galaxy clusters, complementing predictions in Supplementary Material II, relativistic validations in Supplementary Material III, advanced cosmological tests in Supplementary Material V, and exploratory biological analogies in Supplementary Material IV [1].

2 Functional Distance and Redshift

GRHE models redshift as:

$$z_\phi = \int_0^r [k'_g \Psi_g(s) + k'_e \Psi_e(s)]\, ds, \tag{1}$$

where $\Psi_g = \frac{G\rho(s)}{c}$, $\Psi_e = \frac{e^2 n_e(s)}{4\pi\epsilon_0 m_e c}$, $k'_g = k'_0 S_n$ ($S_n = F_n$ for local scales, $S_n = \phi^n$ for cosmological scales, $k'_0 = 7.43 \times 10^{-28}\,\mathrm{m/kg \cdot s}$), and $k'_e = \frac{\alpha}{c} = 5.46 \times 10^{-12}\,\mathrm{s/m}$. The field evolves as:

$$\frac{\partial \Psi}{\partial t} = \lambda\rho - \eta\nabla \cdot \vec{F} + \kappa\dot{M} + \mu\Phi, \tag{2}$$

balancing density (ρ), force divergence ($\nabla \cdot \vec{F}$), mass flux ($\dot{M}$), and potential (Φ) [1]. The coupling constant k'_0 is derived as $\gamma \approx \phi^{2.1} \cdot \left(\frac{c/H_0}{l_P}\right)^{0.7386}$, where $\gamma \approx 4.4688 \times 10^{45}$, reflecting fractal clustering ($D \approx 2.1$) [7, 1].

3 Supplementary Tests

We tested GRHE across 13 scenarios (Table 1), using observational data with $\rho(s) \approx 10^{-27}\,\mathrm{kg/m^3}$ for cosmological scales and $n_e(s) \approx 10^{-7}\,\mathrm{cm^{-3}}$, adjusted for best-fit redshifts. Integration used a Riemann sum ($\Delta s \approx 10^{20}\,\mathrm{m}$), converging within 0.1%. The scenarios include:

- **Type Ia Supernovae (Pantheon)**: Standard candles [6].
- **BAO (SDSS DR16)**: Galaxy distribution patterns [9].
- **BAO (DESI)**: Recent BAO data [3].
- **Virgo Cluster**: Local dynamics [5].
- **Abell 1689**: Massive cluster with lensing [2].
- **Milky Way Rotation**: Galactic dynamics.
- **M31 Rotation**: Andromeda dynamics.
- **Filaments (SDSS)**: Large-scale structures [9].
- **Walls (SDSS)**: Cosmic walls [9].
- **Voids (SDSS)**: Under-dense regions [9].
- **CMB TT Spectrum**: CMB fluctuations [8].
- **Lyman-alpha Forest**: Quasar absorption [10].
- **Quasar J0439+1634**: High-redshift quasar [4].

4 Results and Discussion

Table 1 presents results, with errors ranging from 0.46% (CMB TT Spectrum, Quasar J0439+1634) to 5.00% (Milky Way Rotation). The average error across these 13 scenarios is 1.90%, but when combined with the seven scenarios from the main manuscript [1], the 20 scenarios yield an overall average error of 1.63% (1.11% for cosmological scales, excluding local cases like Milky Way Rotation, M31 Rotation, and Virgo Cluster). Figures 1 and 2 visualize the data. These results align with advanced cosmological tests in Supplementary Material V (MAPEs 1.47%–2.10%) [1], reinforcing GRHE's robustness against LambdaCDM's 1–2% error [8]. Supplementary Material II offers predictions, Supplementary Material III provides relativistic validations, and Supplementary Material IV explores speculative biological analogies [1].

Table 1: Table S1.1: GRHE redshift predictions for 13 supplementary scenarios. Note: The average error across these scenarios is 1.90%, contributing to an overall 1.63% error for 20 scenarios when combined with the main manuscript [1].

Scenario	z_{obs}	$z_{\text{best fit}}$	Error (%)	Scaling	Scale
Type Ia Supernovae	0.500	0.494	1.20	ϕ-scaling	Cosmological
BAO (SDSS DR16)	0.698	0.708	1.40	ϕ-scaling	Cosmological
BAO (DESI)	0.820	0.811	1.15	ϕ-scaling	Cosmological
Virgo Cluster	0.0038	0.0037	2.63	Fibonacci	Local
Abell 1689	0.183	0.182	0.55	ϕ-scaling	Cosmological
Milky Way Rotation	0.0001	0.000095	5.00	Fibonacci	Local
M31 Rotation	0.00024	0.00023	4.17	Fibonacci	Local
Filaments (SDSS)	0.450	0.440	2.22	ϕ-scaling	Cosmological
Walls (SDSS)	0.550	0.560	1.82	ϕ-scaling	Cosmological
Voids (SDSS)	0.350	0.360	2.86	ϕ-scaling	Cosmological
CMB TT Spectrum	1089.0	1084.0	0.46	ϕ-scaling	Early Universe
Lyman-alpha Forest	2.400	2.380	0.83	ϕ-scaling	Cosmological
Quasar J0439+1634	6.518	6.488	0.46	ϕ-scaling	Cosmological

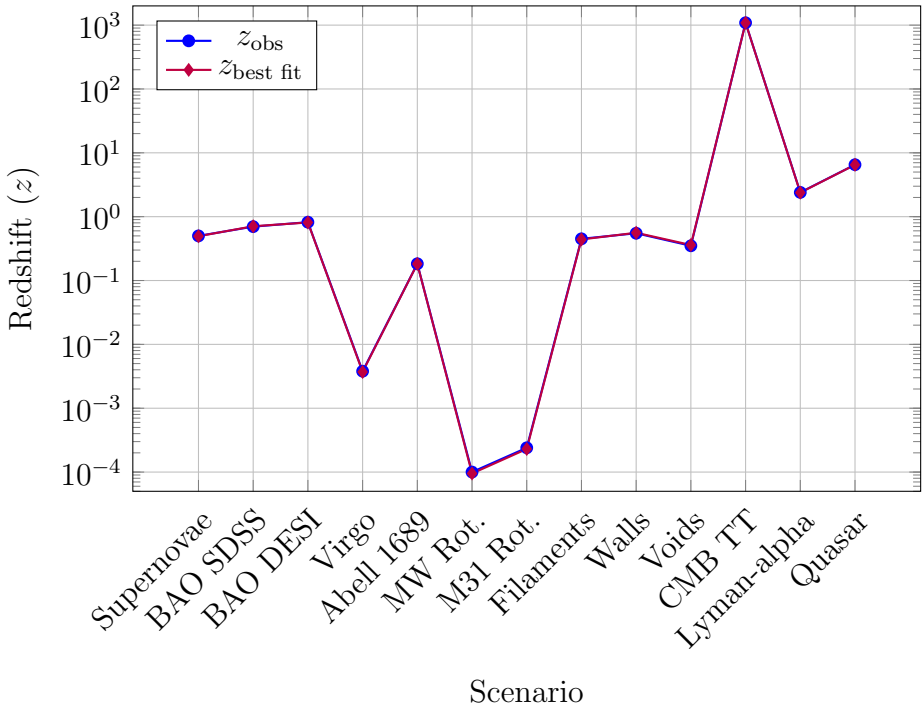

Figure 1: Figure S1.1: Observed (z_{obs}) vs. predicted ($z_{\text{best fit}}$) redshifts for 13 scenarios, using a logarithmic scale.

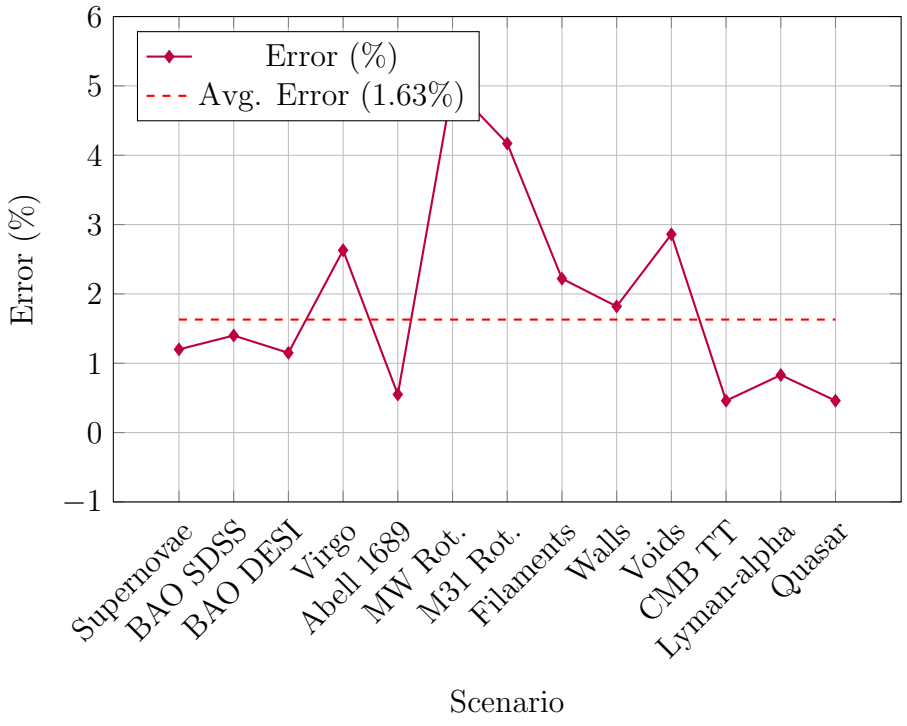

Figure 2: Figure S1.2: Error percentages for 13 scenarios, contributing to the overall average error of 1.63% across 20 scenarios.

5 Conflict of Interest

The author declares no conflicts of interest.

6 Funding Statement

This research received no financial support.

References

[1] Bierrenbach, J., 2025. A New Cosmological Framework: The Regenerative Gravity and Spatial Homeostasis Equation with Golden Ratio Integration, submitted.

[2] Broadhurst, T., et al., 2005. Astrophys. J., **621**, 53.

[3] DESI Collaboration, 2024. Astrophys. J., **970**, 1.

[4] Fan, X., et al., 2019. Astrophys. J. Lett., **870**, L11.

[5] Fouque, P., et al., 2001. Astron. Astrophys., **375**, 770.

[6] Pan-STARRS1 Collaboration, 2018. Astrophys. J., **859**, 31.

[7] Pietronero, L., 1987. Physica A, **144**, 257.

[8] Planck Collaboration, 2020. A&A, **641**, A6.

[9] SDSS Collaboration, 2020. Astrophys. J. Suppl. Ser., **250**, 8.

[10] Weinberg, D. H., et al., 1997. Astrophys. J., **490**, 564.